

PAPER • OPEN ACCESS

Improving the ripple classification in focal pediatric epilepsy: identifying pathological high-frequency oscillations by Gaussian mixture model clustering

To cite this article: Carolina Migliorelli *et al* 2021 *J. Neural Eng.* **18** 0460f2

View the [article online](#) for updates and enhancements.

You may also like

- [Exploring the time–frequency content of high frequency oscillations for automated identification of seizure onset zone in epilepsy](#)
Su Liu, Zhiyi Sha, Altay Sencer et al.
- [Automated detection of epileptic ripples in MEG using beamformer-based virtual sensors](#)
Carolina Migliorelli, Joan F Alonso, Sergio Romero et al.
- [Long term evolution of fast ripples during epileptogenesis](#)
Mariam Al Harrach, Pascal Benquet and Fabrice Wendling



PAPER

OPEN ACCESS







RECEIVED
19 March 2021REVISED
15 July 2021ACCEPTED FOR PUBLICATION
12 August 2021PUBLISHED
31 August 2021

Original content from this work may be used under the terms of the [Creative Commons Attribution 4.0 licence](https://creativecommons.org/licenses/by/4.0/).

Any further distribution of this work must maintain attribution to the author(s) and the title of the work, journal citation and DOI.



Improving the ripple classification in focal pediatric epilepsy: identifying pathological high-frequency oscillations by Gaussian mixture model clustering

Carolina Migliorelli^{1,2,3,*} , Sergio Romero^{1,2,3} , Alejandro Bachiller^{2,3} , Javier Aparicio⁴,
Joan F Alonso^{1,2,3} , Miguel A Mañanas^{1,2,3}  and Victoria San Antonio-Arce^{4,5} 

¹ CIBER de Bioingeniería, Biomateriales y Nanomedicina (CIBER-BBN), Madrid, Spain

² Universitat Politècnica de Catalunya, Department of Automatic Control (ESAI), Biomedical Engineering Research Centre (CREB), Barcelona, Spain

³ Institut de recerca pediàtrica Hospital Sant Joan de Déu, Barcelona, Spain

⁴ University Hospital Sant Joan de Déu, Epilepsy Unit. Department of Neuropediatrics (member of the European Reference Network for rare and complex epilepsies EpiCARE), Barcelona, Spain

⁵ Freiburg Epilepsy Center, Medical Center—University of Freiburg, Faculty of Medicine (member of the European Reference Network for rare and complex epilepsies EpiCARE), Freiburg, Germany

* Author to whom any correspondence should be addressed.

E-mail: Carolina.migliorelli@upc.edu

Keywords: stereo-EEG, Epilepsy, high-frequency oscillations, ripple band, presurgical assessment

Supplementary material for this article is available [online](#)

Abstract

Objective. High-frequency oscillations (HFOs) have emerged as a promising clinical biomarker for presurgical evaluation in childhood epilepsy. HFOs are commonly classified in stereo-encephalography as ripples (80–200 Hz) and fast ripples (200–500 Hz). Ripples are less specific and not so directly associated with epileptogenic activity because of their physiological and pathological origin. The aim of this paper is to distinguish HFOs in the ripple band and to improve the evaluation of the epileptogenic zone (EZ). **Approach.** This study constitutes a novel modeling approach evaluated in ten patients from Sant Joan de Deu Pediatric Hospital (Barcelona, Spain), with clearly-defined seizure onset zones (SOZ) during presurgical evaluation. A subject-by-subject basis analysis is proposed: a probabilistic Gaussian mixture model (GMM) based on the combination of specific ripple features is applied for estimating physiological and pathological ripple subpopulations. **Main Results.** Clear pathological and physiological ripples are identified. Features differ considerably among patients showing within-subject variability, suggesting that individual models are more appropriate than a traditional whole-population approach. The difference in rates inside and outside the SOZ for pathological ripples is significantly higher than when considering all the ripples. These significant differences also appear in signal segments without epileptiform activity. Pathological ripple rates show a sharp decline from SOZ to non-SOZ contacts and a gradual decrease with distance. **Significance.** This novel individual GMM approach improves ripple classification and helps to refine the delineation of the EZ, as well as being appropriate to investigate the interaction of epileptogenic and propagation networks.

1. Introduction

High-frequency oscillations (HFOs) have emerged as a promising clinical biomarker for helping in the identification of the epileptogenic zone (EZ), defined as the brain area indispensable for seizure generation [1]. In refractory childhood epilepsy, the top priority is the selection of the most appropriate treatment for each child [2]. In this sense, individualized HFOs

study provides new insights into personalized presurgical evaluation [3]. Resection of areas with high HFO rates is associated with good postsurgical outcome [1, 4, 5]. HFOs are defined as fast spontaneous transient events with at least four oscillations above 80 Hz that stand out from baseline [6]. HFOs are classified into ripples (80–200/250 Hz) and fast ripples (200/250–500 Hz) [7]. The recommended sampling frequency for signal acquisition is at least four to five

times the highest frequency of interest [8]. Hence, frequencies higher than 1 kHz and 2 kHz are required to identify ripples and fast ripples, respectively [9], leading to large storage, high processing, and extended computation time requirements for long-term intracranial EEG recordings [10]. For this reason, recent studies are still focused on the ripple band [11–13].

High-frequency activity occurs not only in the epileptogenic cortex, but also in normal cortical areas [14, 15]. Ripples are more frequently noticed both as a pathological and physiological phenomenon than fast ripples [16], which are more specifically elicited by epileptogenic tissues [17]. On one side, many cognitive, visual or motor tasks generate physiological HFOs [18–20]. On the other, pathological HFOs are mostly generated in the seizure onset zone (SOZ) but they propagate outside [21, 22]. Consequently, their distinction is still challenging [23]. Large clinical studies have shown too high a variability of HFO rates to establish a global threshold, and there is no guarantee that channels with the highest rates indicate the resection area to achieve seizure freedom. Differences in rate can also occur due to the presence of physiological oscillations, different electrode types and SOZ location [4].

Previous studies have assessed this issue focusing on the statistical differences in features from ripples inside and outside the SOZ [20, 24, 25], considering as pathological all spontaneous ripples inside the SOZ recorded interictally or preictally. The most discriminant features from these studies were the amplitude and the instantaneous frequency. Ripples inside the SOZ showed statistically significant higher amplitudes and lower instantaneous frequencies. However, physiological ripples such as those of the hippocampus have features overlapping with those of pathological ones [4]. Probably, this is caused by global classification approach that applies the same feature boundaries to all patients, and due to not considering the simultaneous presence of pathological and physiological ripples [26, 27].

The aim of this paper is to present a novel approach to separate pathological and physiological HFOs in the ripple band in a retrospective study with pediatric patients suffering from focal epilepsy. For this, we propose (a) a subject-by-subject analysis without spatial constraints; (b) a probabilistic Gaussian mixture model (GMM) based on the combination of several features; and (c) the estimation of the physiological and pathological ripple subpopulations within the overall HFO distribution of each patient.

This novel individual GMM approach can help to: (a) refine the delineation of the pathologic HFO zone, even with data without epileptiform activity, checking the increased rates inside the SOZ versus outside; (b) investigate the interaction of epileptogenic and propagation networks.

2. Materials and methods

2.1. Database description and acquisition settings

A proof of concept was evaluated in ten pediatric patients diagnosed with intractable epilepsy at Sant Joan de Déu Barcelona Children's Hospital with a suspicion of a single epileptic generator. All subjects gave informed consent and the study was approved by the ethical committee of the same Hospital. Table 1 shows a summary of the available clinical information. Eight out of the ten patients achieved seizure freedom after surgery.

Stereoelectroencephalography (SEEG) signals were acquired using a referential montage (reference in the white matter) during 7.16 (± 1.34) days using a Micromed system with 1024 Hz sample frequency (400 Hz bandwidth) and DIXI depth electrodes implanted stereotactically. Simultaneous scalp EEG was recorded from electrodes on the midline sagittal plane (Fz, Cz, Pz).

Aided by the scalp EEG, SEEG corresponding to a 30 min period of slow-wave sleep interictal activity of the first night of each patient was selected for further analysis. At that time, changes in medication were minor, no previous seizure had been recorded and no electrical stimulation had been performed. Segments were considered as interictal if they were at least 1 h away from subtle seizures and 8 h from focal to bilateral tonic-clonic seizures. Two experienced epileptologists thoroughly examined these epochs, low-pass filtered to 45 Hz, and scored the sections characterized by low-frequency interictal epileptiform activity (IEA). The same experts defined the SOZ visually, identifying the channels with early ictal discharges on the long-term video SEEG recordings.

2.2. HFOs detection

The SGM algorithm was used to detect HFOs in the ripple band (80–200 Hz). SGM is already published and was validated using simulated and real data assessed by two experts [28]. Briefly, the algorithm consists of: (a) baseline estimation using the entropy of the autocorrelation; (b) S-Transform [29] to calculate time-frequency features; and (c) GMM-based clustering of the features to decide if events are HFO-like activity. The detected HFOs were treated as independent events on a channel-by-channel basis.

The HFO rate was obtained as the number of HFOs per minute for each channel, and the density was the ratio between the duration of all HFOs and the duration of the segments. This calculation was performed for the whole available 30 min signal, and IEA and non-IEA segments separately. Because rate and density showed comparable results, only rate results are shown.

Table 1. Clinical information of patients included in the study. All patients were right-handed.

Patient	Age	Sex	Medication ^a	SOZ	SEEG implantation (month-year)	N° channels	N° channels SOZ	% Epileptiform activity	Surgery/Pathology ^b	Seizure freedom
1	18	F	CBZ, LEV	Occipital lateral	15 Nov	94	4	13.14	Complete resection/ Ganglioglioma WHO grade I + FCD IIIb	Yes, Engel Ia (4 years post-surgery)
2	10	M	CBZ, VPA, PB	Frontal pre-motor lateral	16 Apr	68	6	19.17	Incomplete resection/ FCD II a	Yes, Engel Ic (3 years post-surgery) Does not apply
3	9	F	CBZ, LCM	Pre-central	17 Jan	78	4	21.88	Not performed (SOZ overlapped motor area)	
4	8	M	CLB	Amygdala	16 Sep	109	4	16.52	Complete resection/ Ganglioglioma WHO grade I + FCD IIIb	Yes, Engel Ia (3 years post-surgery)
5	9	M	CBZ, ZNS	Frontal pre-motor lateral	16 Jun	97	10	21.76	Complete resection/ FCD IIb	Yes, Engel Ia (6 months post second surgery) Yes, Engel IIb (3 months post-second surgery) ^b
6	9	M	CBZ, CLB, LCM, LEV	Temporal antero-mesial + insula + fronto-basal	16 May	72	5	17.57	Incomplete resection/ Ganglioglioma WHO grade I + FCD IIIb	No, Engel IIIa (3 years post-surgery)
7	5	F	VPA, TPM, LCM	Temporo-parieto-occipital	17 Feb	94	4	8.49	Complete disconnection/ Ischemic lesion ^c	
8	16	M	CBZ, CLB, LEV, PER, LCM	Parietal	17 Apr	101	6	7.77	Incomplete resection/ Polimicrogyria	Yes, Engel IVa (2 years post-surgery)
9	7	F	LEV, PER	Temporal antero-mesial	17 May	79	7	8.11	Complete resection/ FCD II a	Yes, Engel Ia (2 years post-surgery)
10	17	M	LCM, PER, VPA	Frontal lateral	17 Sep	120	8	17.55	Complete resection/ FCD II a	Yes, Engel Ia (1 year post-surgery)

^a Medications codes: CBZ: Carbamazepine, LEV: Levetiracetam, VPA: Valproate, PB: Phenobarbital, LCM: Lacosamide, ESL: Eslicarbazepine, CLB: Clobazam, ZNS: Zonisamide. * FCD: Focal cortical dysplasia.

^b Second surgery in SID.

^c SOZ is probably hemispheric.

2.3. HFO feature extraction

Previous studies have reported amplitude and instantaneous frequency as the most discriminant features between SOZ and non-SOZ [20, 24, 25]. After performing the detection with the SGM algorithm, we calculated these features from each detected HFO in the band-pass filtered signal (80–250 Hz, using a finite impulse response filter of 80th order).

- *Instantaneous frequency*, the inverse of the average oscillation period (between-peaks time).
- *Amplitude*, the maximum value of the envelope, computed by the Hilbert transform.

2.4. Clustering pathological and physiological ripples and statistical analysis

The selected features were log-scaled to reduce skewness and used to fit a two-cluster GMM, using a full-covariance matrix. An independent model was fitted to each patient and to each feature to soft-cluster ripples into two groups: pathological and physiological. HFOs were labeled as clearly pathological if both membership probabilities (high-amplitude cluster and low-frequency cluster) exceeded 50%. On the other hand, clearly physiological ripples were identified when both membership probabilities were lower than 50%, that is, low-amplitude and high-frequency HFOs. The ripples that did not meet these criteria were considered as undefined.

To evaluate the differences in rates inside and outside the SOZ an independent t-test was used (significance set to 5%). To compare both groups, SOZ and non-SOZ were normalized by dividing their mean rate by the number of channels that compose them.

2.5. Pathological ripples as a delimiter of the SOZ

One of the most evident uses of the detection of clearly pathological ripples is the delineation of the pathological ripple zone and its overlapping with the SOZ. The channels with higher pathological ripple rates are expected to be located inside the SOZ, markedly linked with the epileptogenic process. We define the pathological ripple zone as the contacts with the pathological HFO rate exceeding a certain percentile. To determine the most suitable value, percentiles from 50 to 95, in steps of 5, were considered. For each measurement, the following quantities were defined:

- True positive (TP): number of channels belonging to the SOZ exceeding the percentile.
- False positive (FP): number of channels not belonging to the SOZ exceeding the percentile.
- True negative (TN): number of channels not belonging to the SOZ and not exceeding the percentile.
- False negative (FN): number of channels belonging to the SOZ but not exceeding the percentile.

The following performance measures were analyzed for each considered percentile value:

$$\text{Sensitivity} = \frac{TP}{TP + FN} \quad (1)$$

$$\text{Specificity} = \frac{TN}{TN + FP} \quad (2)$$

$$\text{Accuracy} = \frac{TP + TN}{TP + TN + FP + FN}. \quad (3)$$

2.6. Data availability

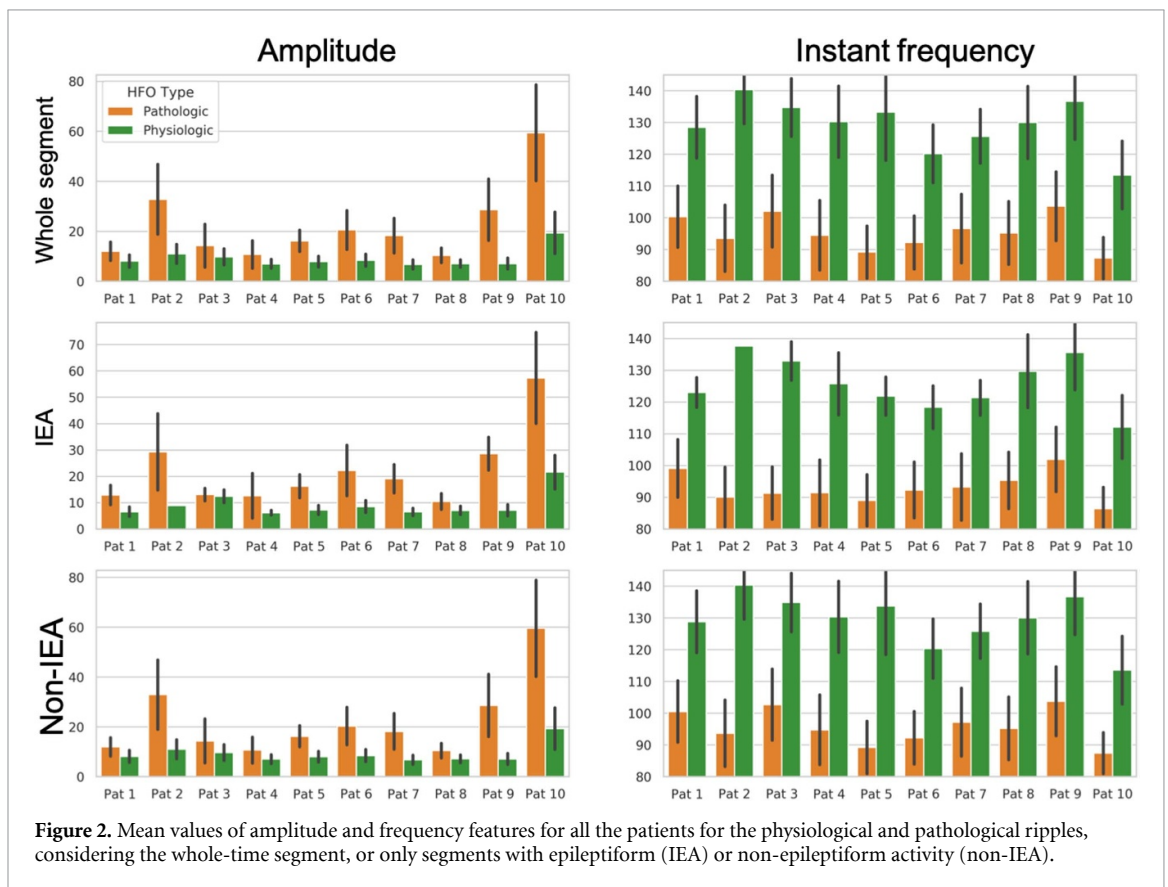
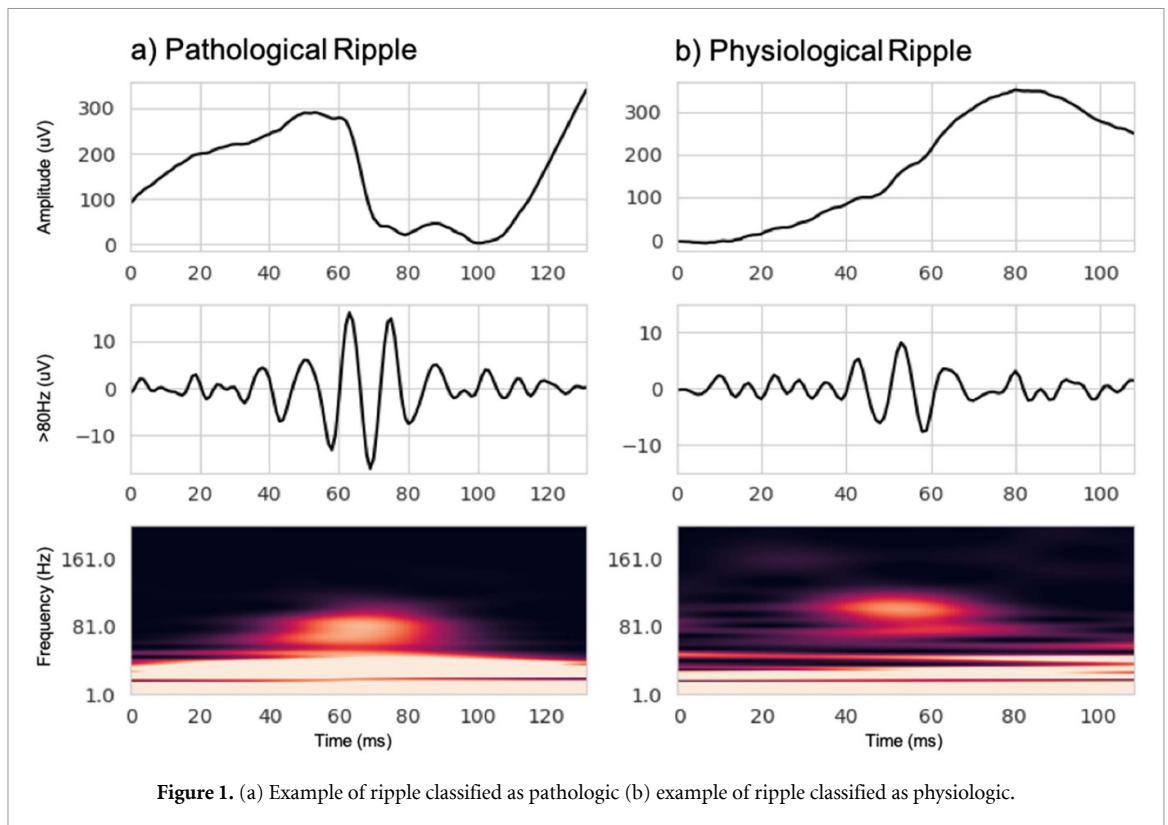
The conditions of our ethical approval do not allow public archiving of anonymized patient data. Derived data supporting the findings are available on reasonable request from the corresponding author. The SGM algorithm [28] is implemented in Python and freely-available (<https://github.com/cmiglio/epyHFO>).

3. Results

3.1. Classification between physiological and pathological ripples

Once HFOs were detected for each patient using SGM, independent GMMs were fitted to each subject and feature (amplitude and instantaneous frequency) to obtain clearly pathological and physiological groups that contained events whose features were more distinctive. For ease of reference, the clearly pathological and clearly physiological groups are hereinafter labeled as pathological and physiological, respectively. Figure 1(a) shows, as an example, a pathological and a physiological ripple. Both time and time-frequency representations are similar, being different only in the amplitude above 80 Hz (higher for pathological) and the instantaneous frequency (lower for pathological). The distributions of the features used by the SGM detector (area, entropy, time width and frequency width) [28] did not show statistically significant differences between groups, indicating that the time-frequency pattern was similar for all the ripples.

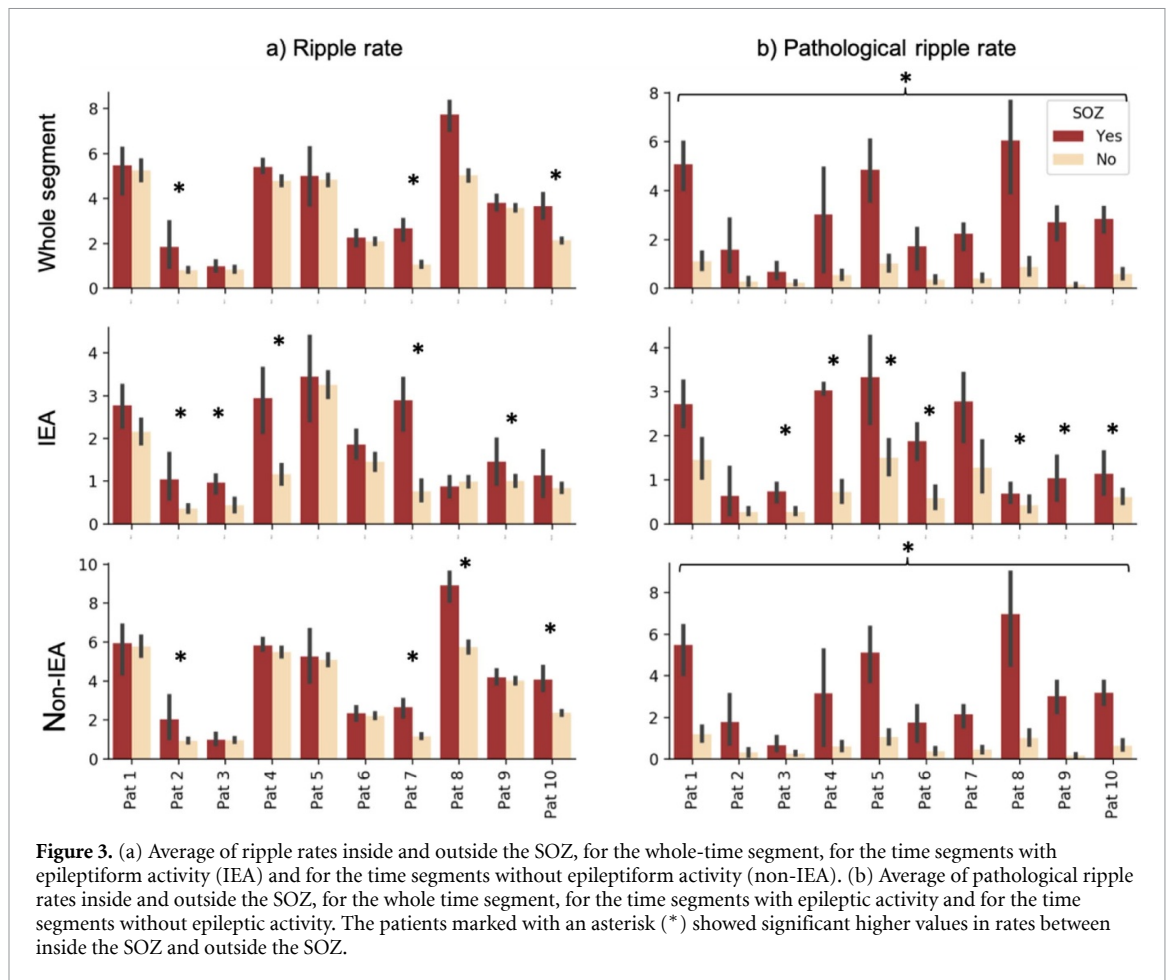
Figure 2 shows the average amplitude and instantaneous frequency for each subject considering the whole SEEG segment, and IEA and non-IEA segments separately. Features remained similar whether epileptiform activity was present or not, suggesting that ripple characteristics depend on their pathological or physiological nature but not on the presence of low-frequency epileptiform activity. The high between-subject variability (especially in amplitudes) that hinders the estimation of global boundaries between pathological and physiological ripples is remarkable. For example, physiological ripples of patient 10 have similar amplitudes to pathological ripples of patient 6 and 7.



3.2. Occurrence of pathological ripples

Figure 3(a) shows the overall ripple rates inside and outside the SOZ for each patient, considering the whole segment, only IEA, and only non-IEA

segments. In the first case, rates were statistically higher inside the SOZ in four patients. Considering the IEA segments, five patients showed statistical differences. And in non-IEA segments four patients



showed significantly higher rates inside the SOZ. Note that 40% of the patients showed similar rates inside and outside the SOZ if no separation between pathological and physiological was performed.

Figure 3(b) shows pathological ripple rates inside and outside the SOZ. These were significantly higher in the SOZ than outside for all patients. While averaged ratios between SOZ and non-SOZ rates were 1.01 ± 0.45 , ratios increased to 5.42 ± 2.98 when only pathological ripples were considered. Pathological ripples co-occurring in time with other low-frequency IEA showed a significantly higher rate inside SOZ for most patients (3, 4, 5, 6, 8, 9 and 10) whereas pathological ripples not accompanied of IEA, showed statistically higher values for all the patients.

These rates correspond to grand averages of all channels, whose count differed outside and inside the SOZ. Figure 4 shows the rates for all channels and patients, sorting channels in descending rate order, in three cases: all the ripples, only pathological, and only physiological. Considering all ripples, the highest-rate channels did not belong to the SOZ in half of the patients (1, 3, 4, 6, 9) and in the other half some SOZ channels did not exhibit the highest rates. In contrast, considering the pathological ripples only, the highest rates were mostly in SOZ channels, and rates decreased more dramatically. Physiological ripples

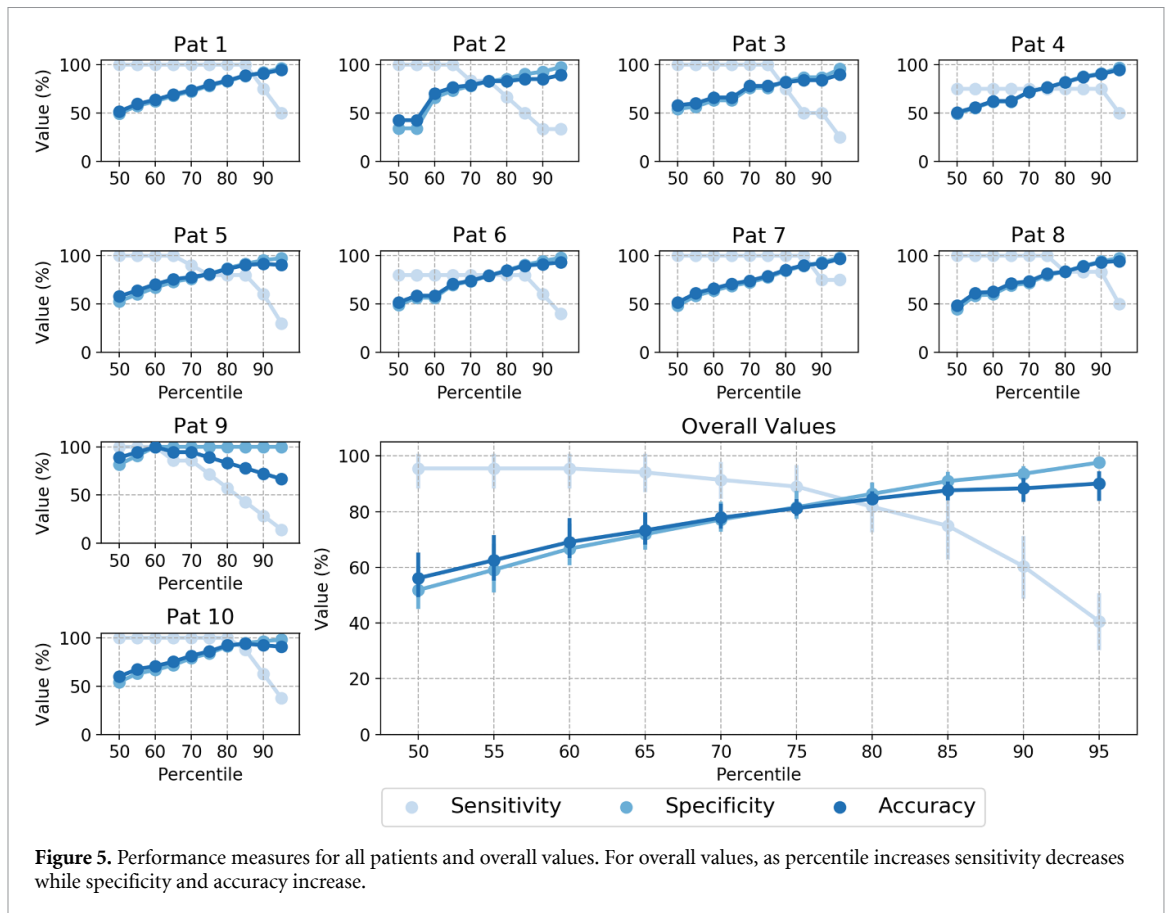
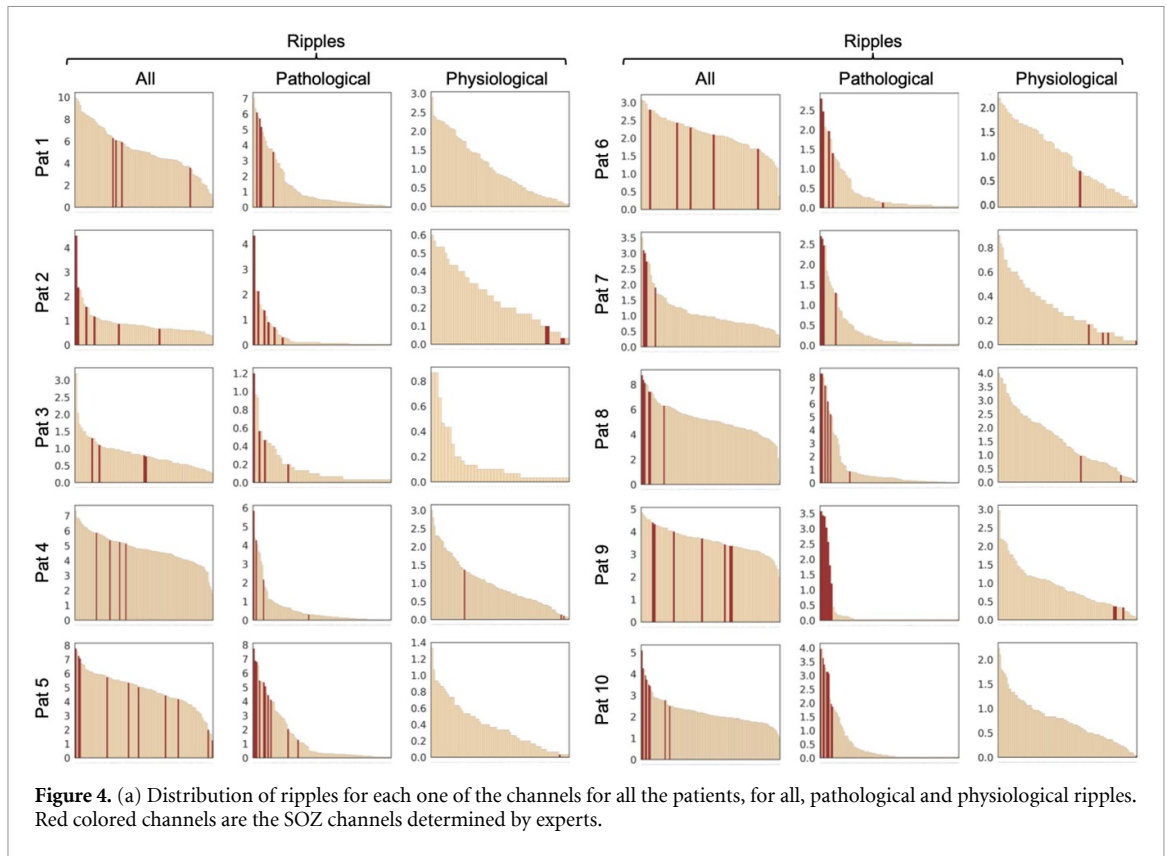
were distributed into more channels and mainly outside the SOZ.

3.3. Performance of pathological ripples as a delimiter of the SOZ

Sensitivity, specificity and accuracy were computed for percentile values from 50 to 95. Figure 5 shows these measures for each patient as well as overall mean and standard deviation. For overall values, the optimal value is around 75 and 80: for the percentile 75 the values obtained were a sensitivity of 88.98% (71.43%–100%), a specificity of 81.58% (76.09%–100%), and an accuracy of 81.22% (76.34%–88.89%). For the percentile 80, sensitivity was 81.71% (57.14%–100%), specificity 86.4% (82.02%–100%), and accuracy of 84.57% (81.72%–92.31%).

3.4. Pathological ripples outside the SOZ

As expected, the percentage of pathological ripples was much higher inside than outside the SOZ. However, pathological ripples outside the SOZ distributed heterogeneously among patients. Most patients showed a low number of pathological ripples outside the SOZ, but patients 1, 3 and 5 presented a substantial number of pathological ripples outside the SOZ (see figures 3 and 4). For each patient, the percentage change in rates with respect to the



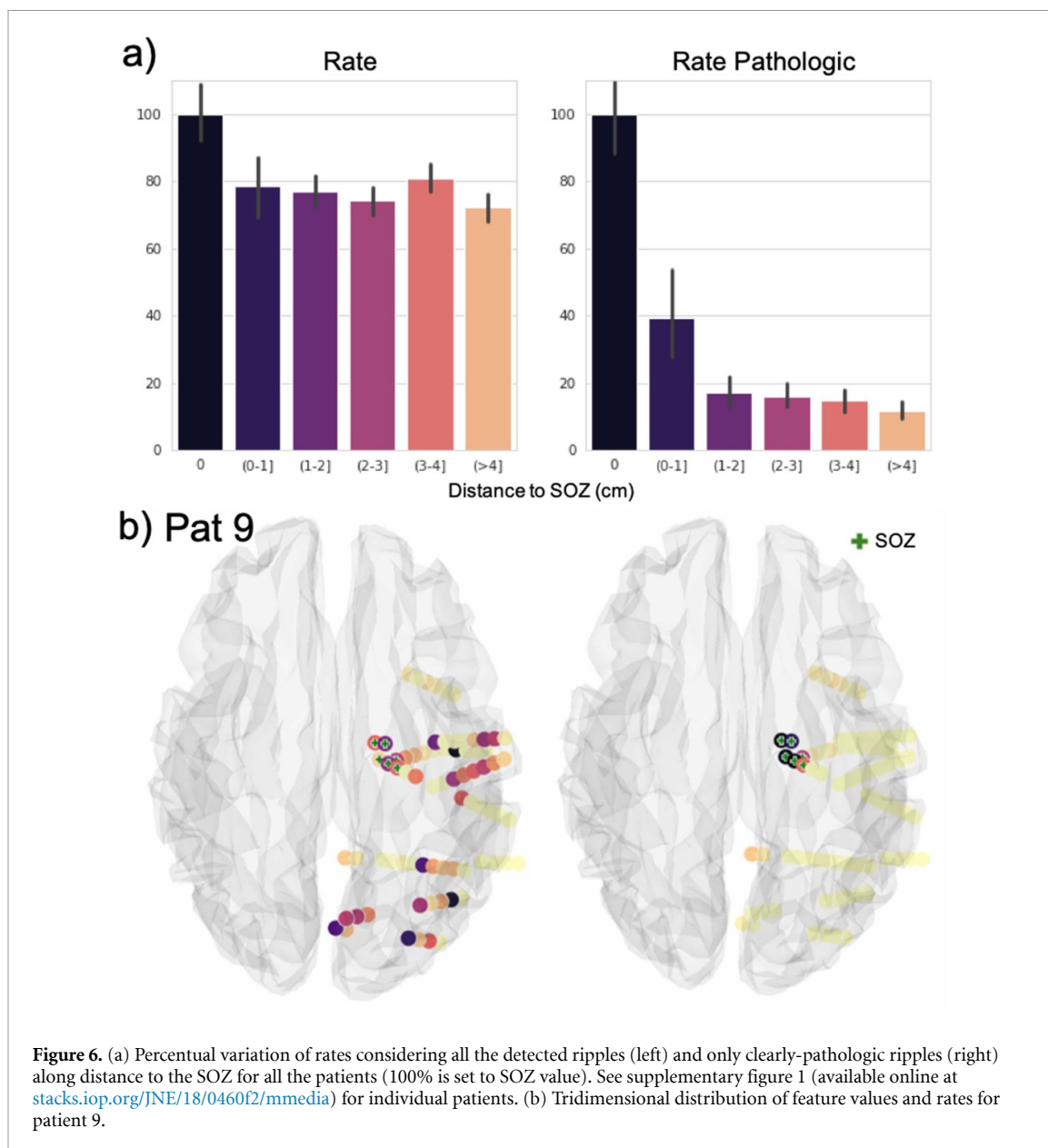


Figure 6. (a) Percentual variation of rates considering all the detected ripples (left) and only clearly-pathogenic ripples (right) along distance to the SOZ for all the patients (100% is set to SOZ value). See supplementary figure 1 (available online at stacks.iop.org/JNE/18/0460f2/mmedia) for individual patients. (b) Tridimensional distribution of feature values and rates for patient 9.

SOZ (100% being the SOZ) was computed by grouping electrodes by distance to the SOZ. Figure 6(a) shows the change with distance (from the nearest to the furthest group) for all the patients. The effect of distance on HFO rates was observed, but only for pathological ripples the rate showed a steep decline between SOZ and non-SOZ and a gradual decline with increasing distance. This was not observed if all ripples or only physiological ones were considered.

Figure 6(b) shows, as an example, the ripple rate tridimensional spatial distribution of patient 9. Considering all ripples, the SOZ region (contacts with a green cross) showed high rates (darker colors) but also other regions; therefore the high-rate area was more widespread. Considering only the pathological ripples, the highest rate channels appeared in a narrower area.

4. Discussion

In the recent years, the differentiation between physiological and pathological HFOs has generated considerable debate. Whereas pathological HFOs are more specific to the epileptogenic tissue, physiological HFOs occur across different brain areas, mostly in the occipital and temporal cortex [30]. Still, pathological HFOs can also be recorded outside the SOZ mainly due to propagation.

Among HFO characteristics, the fast ripple rate is significantly increased in the SOZ and seems to provide better post-surgical outcomes in terms of seizure freedom [31]. However, fast ripples require high sampling rates [6, 9] that are not common in clinical practise, making ripple analysis very interesting [11–13]. Ripple activity, however, is abundant in both epileptogenic and physiological brain areas and

its usefulness to delineate the EZ has been questioned [3, 32].

In all patients, especially pediatric, the reduction in time of the invasive presurgical assessment could positively impact children's and their carers' life. Ripple analysis could also be especially useful if seizures fail to be recorded during this assessment.

4.1. Pathological and physiological ripples differentiation and its relationship with the SOZ

The most accepted metrics for the delimitation of SOZ is the rate per channel [5, 27]. In our work, rates were found to be like those reported in other studies [33, 34].

Unlike the fast ripple rate, the ripple rate does not localize the SOZ effectively [16, 27]. In addition, previous studies have shown the difficulty to estimate thresholds to associate rates with the SOZ or not due to the presence of physiological ripples, among others [4]. In our study, when considering all ripples together, ripple rates were statistically higher inside the SOZ only in 4 out of 10 patients. In addition, we found contacts outside the SOZ with similar or even higher HFO rates to those inside the SOZ (see figure 4).

We hypothesized that pathological ripples appear mostly in the SOZ, whereas physiological ripples scatter roughly evenly along contacts inside and outside the SOZ, caused by brain activity not related to epilepsy. Several studies have characterized the HFO activity and reported that ripples in the SOZ had higher amplitude and lower frequency than ripples outside the SOZ [11, 15, 16]. Our results agreed: amplitude and instantaneous frequency showed within-subject statistical differences between inside and outside the SOZ, for all the patients (see figure 3). However, these previous studies showed a considerable overlap between the SOZ and non-SOZ ripple distributions, providing unclear conclusions regarding the determination of the SOZ based on ripple activity. This could be caused by considering the ripples detected inside and outside the SOZ as pathological and physiological, respectively. The purpose of our study was to identify pathological ripples, independently of their localization. By using GMM-based clustering, we achieved a statistically consistent soft classification of ripples into two clusters (clearly pathological and clearly physiological) using the two proposed features. Ripples labeled as clearly pathological by probabilistic membership gathered mostly in the SOZ and exhibited a significant higher rate inside than outside the SOZ for all patients, even during periods without IEA (see figure 3). In addition, only the rate of clearly pathological ripples delimited the SOZ and showed a monotonic decrease with increasing distance from the SOZ (see figure 6), in contrast to the alternative of considering all ripples for the rate

calculation. We hypothesized that this phenomenon reflects the propagation of the some of the pathological ripple activity to other nearby regions, similarly to what happens with low-frequency interictal epileptiform discharges.

Another clearly physiological group was identified by an opposite probabilistic membership definition, and an undefined ripple group remained, including all the events overlapping in the feature space, which might introduce noise to subsequent evaluation. The uncertainty introduced by this undefined group could have hindered the achievement of better results and the conclusions in previous studies. In our work, we considered it not necessary to estimate all the pathological ripples to help delineate the SOZ. Eight out of ten patients included in this study presented successful surgery outcomes, a fact that indicates that the region was well determined during the presurgical analysis. In the other two cases, surgery was either not possible or incomplete because of the affected brain areas.

One of the main advantages of using soft-clustering methods such as GMM is that these membership probabilities could be lowered to include more events in both groups.

Our main objective was to provide a novel methodology for separating clear pathological from physiological ripples, but the delimitation of the SOZ could also be achieved. Figure 4 shows the ripple rate distribution per channel (all ripples, pathological, and physiological) for all the subjects. The pathological ripple distribution presented a steeper decline in rate, suggesting that pathological ripples cluster around an area composed by a lower number of channels that correlate better with the SOZ. In contrast, this pattern was not observed when analyzing the distribution of either all the detected ripples or the physiological ripples.

Considering different percentile values of pathological ripples in each channel, we measured the sensitivity, specificity and accuracy in detecting the SOZ (see figure 5). Depending on the application the preference would be to be more sensitive or more specific, but a trade-off value was found around percentiles 75 and 80. For these percentiles a mean specificity value of 84.42% (79.78%–100%) a mean sensitivity value of 85.05% (57.14%–100%), and a mean accuracy value of 83.08% (79.57%–89.23%) was found. These values exceed the performance measures reported in the literature, for example Liu *et al* 2018 [25] reported an overall specificity of 63% (20%–87%), a sensitivity of 85% (38%–100%) and an accuracy of 65% (25%–80%). This increase could be explained by the application of unique features boundaries to each patient as well as not considering pathological ripples confined only to the SOZ but also possible in secondary regions.

4.2. Inter-subject variability

We observed different rates and feature distributions among subjects. The heterogeneous nature of the epileptic patients because of different location of the SOZ, age, type of lesion, etc, may be the explanation of the variability in the generation and propagation of ripples.

Due to these heterogeneities, intra-subject feature clustering is especially relevant in HFO analysis [3]. Despite such variability, previous studies have extracted results on the SOZ localization through grouped analysis, reporting significant but subtle differences in average [20, 24, 35]. One of our main contributions in comparison with these studies is the confirmation that performing a subject-by-subject analysis with GMM-based clustering improves ripple discrimination into clearly pathological and clearly physiological. For the definition of both groups, an individual GMM was fitted to each patient, obtaining unique feature boundaries that were especially important because of the high inter-subject feature variability (see figure 2). Despite this variability, the proposed methodology obtained promising results in all cases.

4.3. Concurrency of pathological ripples and low-frequency IEA

There is a high interaction between pathological high-frequency activity, NREM sleep, and low-frequency IEA [36]. That is the reason why it has been recommended to perform HFO analysis during slow-wave sleep (stage N3) with visible waveform abnormalities (epileptiform discharges) [9, 14]. In our study, seven patients showed significant differences between the rates inside and outside the SOZ during IEA, while all the patients showed significant differences when considering only the segments without IEA or the whole data.

According to our promising results, once pathological ripples were separated, the analysis of rather short 30 min recordings could give relevant information leading to a more accurate localization of the pathological ripple zone, independently of the presence of low-frequency IEA.

4.4. Limitations and further work

We found that the analysis of ripples in short time segments can provide valuable information to help infer the EZ in children with focal epilepsy. Long-term studies could help understand the epileptogenic process during different brain states (awake, pre-ictal, ictal) and elucidate the role of ripples in the generation and propagation of epileptic seizures. Additionally, recent studies found that the detection of HFOs is possible in noninvasive recordings [23, 34, 37–39]. Thus, the differentiation between ripples considering a whole-head picture and noninvasive data could answer several questions concerning the generation and propagation of epileptiform activity. Moreover, the epileptic and physiological processes assessed by

noninvasive signals could allow an increase of the available databases and research groups involved in epilepsy research.

It is important to note that we performed the analysis without considering that some of the detected events could be synchronous. A previous study has assessed that the ripple-onset preceding a synchronized and multichannel ripple activity has more value to help infer the EZ, and that the synchronized and multichannel activity reflects the propagation [21]. This information could be used to devise new features that might improve the discrimination between physiological and pathological events, and gain insight to further study the current undefined group.

Our results suggest that interictal pathological ripples present in other brain tissues could represent early-propagation areas elucidating epileptic networks (see figure 4). In this sense, the pathological ripples could be used as a valuable tool to detect seizure propagation pathways. This could be of special interest in pediatric patients, analyzing the time course of these networks and their influence on seizure generation and developmental outcomes.

4.5. Conclusion

Our study provides a simple, fully-automated, unsupervised approach to distinguish pathological and physiological HFOs from a database of pediatric patients with focal epilepsy, relying only on the ripple band. Previous studies aimed to differentiate the characteristics of ripples occurring inside and outside the SOZ. In this study we improve the previous results by not assuming any spatial constraint for the identification of pathological and physiological ripples. By using a limited group of ripples labeled as clearly pathological and exploiting the soft-clustering capabilities of GMMs on a subject-by-subject basis, we were able to obtain valuable information to infer the EZ individually even with data from non-IEA. Our individualized approach overcomes the difficulties posed by the high variability among subjects present in the HFO features, which hinders the estimation of discriminating boundaries.

Data availability statement

The data that support the findings of this study are available upon reasonable request from the authors.

Acknowledgments

C Migliorelli, S Romero, J F Alonso and M A Mañanas are member of CIBER-BBN, an initiative of the Instituto de Salud Carlos III, Spain. A Bachiller and J F Alonso are Serra Hunter Fellows. V San Antonio-Arce and J Aparicio are members of the European Reference Network for rare and complex epilepsies EpiCARE.

Authors contribution

C M, S R, A B, J F A, J A, M A M, and V S A contributed to the conception and design of the study; C M, J A, and V S A contributed to the acquisition and analysis of data; C M and S R drafted the text and prepared the figures.

Funding

This work was supported by Ministry of Science and Innovation (MICIIN), Spain, under Contract PID2020-117751RB-I00.

Conflict of interest

The authors report no competing interests.

Ethical publication statement

This study was approved by Clinical Research Ethics Committee (CEIm) of Sant Joan de Deu Hospital (code:PIC-117-20). The project was conducted following the requisites of the Spanish law 14/2007, of Biomedical research. We confirm that we have read the Journal's position on issues involved in ethical publication and affirm that this report is consistent with those guidelines.

ORCID iDs


Carolina Migliorelli  <https://orcid.org/0000-0003-2781-8841>

Sergio Romero  <https://orcid.org/0000-0002-8627-543X>

Alejandro Bachiller  <https://orcid.org/0000-0001-6507-1027>

Joan F Alonso  <https://orcid.org/0000-0002-2980-6716>

Miguel A Mañanas  <https://orcid.org/0000-0001-9836-6083>

Victoria San Antonio-Arce  <https://orcid.org/0000-0002-2780-6560>

References

- [1] Frauscher B et al 2017 High-frequency oscillations: the state of clinical research *Epilepsia* **58** 1316–29
- [2] Berg A T, Baca C B, Loddenkemper T, Vickrey B G and Dlugos M D 2013 Priorities in pediatric epilepsy research: improving children's futures today *Neurology* **81** 1166–75
- [3] Roehri N, Pizzo F, Lagarde S, Lambert I, Nica A, McGonigal A, Giusiano B, Bartolomei F and Bénar C-G 2018 High-frequency oscillations are not better biomarkers of epileptogenic tissues than spikes *Ann. Neurol.* **83** 84–97
- [4] Remakanthakurup Sindhu K, Staba R and Lopour B A 2020 Trends in the use of automated algorithms for the detection of high-frequency oscillations associated with human epilepsy *Epilepsia* **61** 1553–69
- [5] Modur P and Miodinovic S 2015 Interictal high-frequency oscillations (HFOs) as predictors of high frequency and conventional seizure onset zones *Epileptic Disord.* **17** 413–24
- [6] Jacobs J et al 2012 High-frequency oscillations (HFOs) in clinical epilepsy *Prog. Neurobiol.* **98** 302–15
- [7] Park C J and Hong S B 2019 High frequency oscillations in epilepsy: detection methods and considerations in clinical application *J. Epilepsy Res.* **9** 1–13
- [8] Zijlmans M, Jiruska P, Zelmann R, Leijten F S S, Jefferys J G R and Gotman J 2012 High-frequency oscillations as a new biomarker in epilepsy *Ann. Neurol.* **71** 169–78
- [9] Zijlmans M, Worrell G A, Dümpelmann M, Stieglitz T, Barborica A, Heers M, Ikeda A, Usui N and Le Van Quyen M 2017 How to record high-frequency oscillations in epilepsy: a practical guideline *Epilepsia* **58** 1305–15
- [10] Charupanit K, Sen-Gupta I, Lin J J and Lopour B A 2020 Detection of anomalous high-frequency events in human intracranial EEG *Epilepsia Open* **5** 263–73
- [11] Motoi H, Miyakoshi M, Abel T J, Jeong J-W, Nakai Y, Sugiura A, Luat A F, Agarwal R, Sood S and Asano E 2018 Phase-amplitude coupling between interictal high-frequency activity and slow waves in epilepsy surgery *Epilepsia* **59** 1954–65
- [12] Velmurugan J et al 2018 Magnetoencephalographic imaging of ictal high-frequency oscillations (80–200 Hz) in pharmacologically resistant focal epilepsy *Epilepsia* **59** 190–202
- [13] Pizzo F et al 2017 Epileptogenic networks in nodular heterotopia: a stereoelectroencephalography study *Epilepsia* **58** 2112–23
- [14] Von Ellenrieder N, Dubeau F, Gotman J and Frauscher B 2017 Physiological and pathological high-frequency oscillations have distinct sleep-homeostatic properties *Neuroimage Clin.* **14** 566–73
- [15] Melani F, Zelmann R, Dubeau F and Gotman J 2013 Occurrence of scalp-fast oscillations among patients with different spiking rate and their role as epileptogenicity marker *Epilepsy Res.* **106** 345–56
- [16] Nariai H, Duberstein S and Shinnar S 2018 Treatment of epileptic encephalopathies: current state of the art *J. Child Neurol.* **33** 41–54
- [17] Gliske S V, Irwin Z T, Chestek C, Hegeman G L, Brinkmann B, Sagher O, Garton H J L, Worrell G A and Stacey W C 2018 Variability in the location of high frequency oscillations during prolonged intracranial EEG recordings *Nat. Commun.* **9** 1–14
- [18] Blanco J A et al 2011 Data mining neocortical high-frequency oscillations in epilepsy and controls *Brain* **134** 2948–59
- [19] Cimbáľník J, Hewitt A, Worrell G and Stead M 2018 The CS algorithm: a novel method for high frequency oscillation detection in EEG *J. Neurosci. Methods* **293** 6–16
- [20] Matsumoto A, Brinkmann B H, Stead S M, Matsumoto J, Kuciewicz M T, Marsh W R, Meyer F and Worrell G 2013 Pathological and physiological high-frequency oscillations in focal human epilepsy *J. Neurophysiol.* **110** 1958–64
- [21] Tamlia E, Park E-H, Percivati S, Bolton J, Taffoni F, Peters J M, Grant P E, Pearl P L, Madsen J R and Papadelis C 2018 Surgical resection of ripple onset predicts outcome in pediatric epilepsy *Ann. Neurol.* **84** 331–46
- [22] Wang S, Wang I Z, Bulacio J C, Moshier J C, Gonzalez-Martinez J, Alexopoulos A V, Najm I M and So N K 2013 Ripple classification helps to localize the seizure-onset zone in neocortical epilepsy *Epilepsia* **54** 370–6
- [23] Thomschewski A, Hincapié A-S and Frauscher B 2019 Localization of the epileptogenic zone using high frequency oscillations *Front. Neurol.* **10** 94
- [24] Malinowska U, Bergery G K, Harezlak J and Jouny C C 2015 Identification of seizure onset zone and preictal state based on characteristics of high frequency oscillations *Clin. Neurophysiol.* **126** 1505–13
- [25] Liu S et al 2018 Stereotyped high-frequency oscillations discriminate seizure onset zones and critical functional cortex in focal epilepsy *Brain* **141** 713–30
- [26] Kerber K, Dümpelmann M, Schelter B, Le Van P, Korinthenberg R, Schulze-Bonhage A and Jacobs J 2014 Differentiation of specific ripple patterns helps to identify

- epileptogenic areas for surgical procedures *Clin. Neurophysiol.* **125** 1339–45
- [27] Cimbalnik J, Kucewicz M T and Worrell G 2016 Interictal high-frequency oscillations in focal human epilepsy *Curr. Opin. Neurol.* **29** 175–81
- [28] Migliorelli C, Bachiller A, Alonso J F, Romero S, Aparicio J, Jacobs-Le Van J, Mañanas M A and San Antonio-Arce V 2020 SGM: a novel time-frequency algorithm based on unsupervised learning improves high-frequency oscillation detection in epilepsy *J. Neural. Eng.* **17** 26032
- [29] Stockwell R G 1996 Localization of the complex spectrum: the s transform *IEEE Trans. Signal Process.* **44** 993
- [30] Frauscher B, Von Ellenrieder N, Zelman R, Rogers C, Nguyen D K, Kahane P, Dubeau F and Gotman J 2018 High-frequency oscillations in the normal human brain *Ann. Neurol.* **84** 374–85
- [31] Akiyama T et al 2011 Focal resection of fast ripples on extraoperative intracranial EEG improves seizure outcome in pediatric epilepsy *Epilepsia* **52** 1802–11
- [32] Jacobs J, Wu J Y, Perucca P, Zelman R, Mader M, Dubeau F, Mathern G W, Schulze-Bonhage A and Gotman J 2018 Removing high-frequency oscillations: a prospective multicenter study on seizure outcome *Neurology* **91** e1040–52
- [33] Burnos S, Hilfiker P, Sürücü O, Scholkmann F, Krayenbühl N, Grunwald T and Sarthain J 2014 Human intracranial high frequency oscillations (HFOs) detected by automatic time-frequency analysis *PloS One* **9** e94381
- [34] Migliorelli C, Alonso J F, Romero S, Nowak R, Russi A and Mañanas M A 2017 Automated detection of epileptic ripples in MEG using beamformer-based virtual sensors *J. Neural Eng.* **14** 046013
- [35] Alkawadri R, Gaspard N, Goncharova I I, Spencer D D, Gerrard J L, Zaveri H, Duckrow R B, Blumenfeld H and Hirsch L J 2014 The spatial and signal characteristics of physiologic high frequency oscillations *Epilepsia* **55** 1986–95
- [36] Frauscher B, Von Ellenrieder N, Ferrari-Marinho T, Avoli M, Dubeau F and Gotman J 2015 Facilitation of epileptic activity during sleep is mediated by high amplitude slow waves *Brain* **138** 1629–41
- [37] Von Ellenrieder N, Pellegrino G, Hedrich T, Gotman J, Lina J-M, Grova C and Kobayashi E 2016 Detection and magnetic source imaging of fast oscillations (40–160 Hz) recorded with magnetoencephalography in focal epilepsy patients *Brain Topogr.* **29** 218–31
- [38] Kramer M A et al 2019 Scalp recorded spike ripples predict seizure risk in childhood epilepsy better than spikes *Brain* **142** 1296–309
- [39] Tamilia E, Dirodi M, Alhilani M, Grant P E, Madsen J R, Stufflebeam S M, Pearl P L and Papadelis C 2020 Scalp ripples as prognostic biomarkers of epileptogenicity in pediatric surgery *Ann. Clin. Transl. Neurol.* **7** 329–42